ENEA Centro Ricerche Bologna	Sigla di identificazione	Distrib.	Pag.	di
	ADPFISS – LP1 – 091	L	1	22

Titolo

Molecular Dynamics Approaches to the Determination of MOX Thermophysical Properties

Descrittori

Tipologia del documento: Rapporto tecnico

Collocazione contrattuale: Accordo di programma ENEA-MSE su sicurezza nucleare e reattori di IV generazione

Argomenti trattati: Energia nucleare; Combustibile nucleare; Reattori nucleari veloci

Sommario

MOX fuel is already used in commercial reactors and it is a fundamental issue for the potential deployment of fast breeder reactors. A deep and sound knowledge of the thermo physical properties is crucial for its safe, reliable, and economic use. MD offers a fruitful opportunity for the acquisition of knowledge and competence in a research field of great interest. For the purpose, preliminary actions have been undertaken and presented in this document. In particular, the report provides a review of the MD studies on PuO_2 and MOX fuel, a description of the interatomic potentials applied in the literature, a description of the LAMMPS code that turned out to be a viable option for the continuation of research as preliminary planned in the next PAR 2017.

Il combustibile MOX è già impiegato nei reattori commerciali ed è un elemento fondamentale per il potenziale sviluppo dei reattori veloci. Una conoscenza profonda e solida delle proprietà termofisiche è fondamentale per un utilizzo sicuro, affidabile ed economico. MD offre interessanti opportunità per acquisire conoscenze e competenze in un campo di ricerca di grande interesse. A tal fine, sono state intraprese e presentate in questo documento alcune azioni preliminari. In particolare, il rapporto fornisce una review delle analisi MD sui combustibili PuO_2 e MOX, una descrizione dei potenziali interatomici applicati in letteratura, una descrizione del codice LAMMPS che si è rivelato un'opzione valida per la continuazione di questa linea di ricerca come previsto in via preliminare nel prossimo PAR 2017.

Note

Copia n. **In carico a:**

REV.	DESCRIZIONE	DATA		REDAZIONE	CONVALIDA	APPROVAZIONE
2			NOME			
			FIRMA			
1			NOME			
			FIRMA			
0	EMISSIONE	15.11.2017	NOME	R. Calabrese	F. Rocchi	F. Rocchi
			FIRMA	Rolando Calabrese	Federico Rocchi	Federico Rocchi

TABLE OF CONTENTS

1 INTRODUCTION

The classical molecular dynamics (CMD) simulation of nuclear fuel occupies an important research area between the density functional theory (DFT) and the coarse grained mesoscale models (NEA15). The most important methodologies considered in a Multi-Scale approach to the simulation of nuclear fuel behaviour are presented in Fig. 1.1.

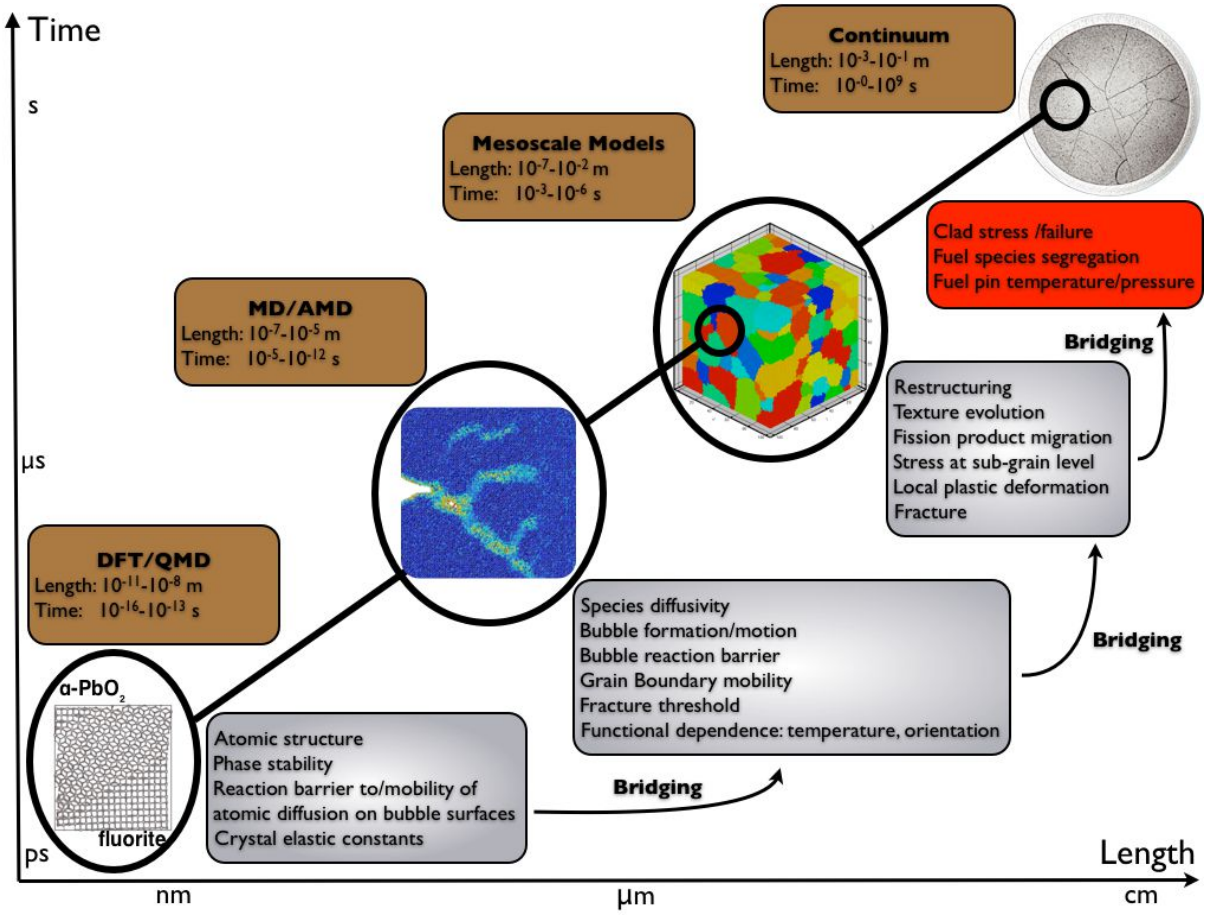

DFT: Density Functional Theory (*ab initio*); QMD: Quantum Molecular Dynamics (electronic structure); MD: Molecular Dynamics (atomistic); AMD: Accelerated MD (atomistic); Mesoscale models: grain-level techniques such as Monte Carlo, Phase Field, Mean Field; Continuum: Finite Element-like techniques.

Figure 1.1: Multi-Scale modelling of nuclear fuel behaviour (NEA15).

Thanks to its capabilities, MD gives the opportunity to study relevant phenomena for the description of the thermo-mechanical behaviour of nuclear fuel such as:

- thermal-mechanical properties;
- radiation damage;

- fission gas bubbles formation/resolution;
- dislocation loops formation/motion;
- grain boundary motion;
- fuel densification.

With regard to PuO_2 and MOX fuel, the efforts of the scientific community have been mostly devoted to develop proper interatomic potentials for the description of the thermophysical properties. In comparison with UO_2, the development of MOX fuel simulations is somehow constrained by the scarce experimental data that makes difficult the assessment of results (e.g., thermal conductivity). The relevance of the methodology for the development of nuclear performance codes is acknowledged. For example, the analysis of the resolution coefficient that is a key parameter in fission gas release models could be an achievable objective of MD (Uff15).

As aforementioned, interatomic potentials play a central role in CMD. This function describes the force field acting between the atoms/ions of the system under consideration. They are analytical functions whose parameters are usually set to predict with good accuracy the available experimental data (e.g., lattice parameter and thermal expansion, bulk modulus). The determination of the parameters could be based on *ab initio* calculations.

A number of well-established classical MD tools can be applied for the simulation of very large number of atoms (e.g., LAMMPS, CHARM, DL_POLY, NAMD, MOLDY (Ack11)). The review has shown that the MXDRTO code has been used in the majority of the references presented here. Beside this, the MOLDY and LAMMPS codes are the most frequently used.

A Molecular Dynamics simulation consists of the numerical step-by-step solution of the classical equations of motion. Atoms basically interact with each other through van der Waals attractive forces, short-range repulsive forces, and electrostatic forces. If they are covalently bonded, strong forces hold them together as stable chemical groups. Position, velocity and acceleration of each atom are calculated using numerical methods (e.g. Verlet method, Runge-Kutta method) to solve the Newton's equations of motion (Bin04). From this microscopic information a series of macroscopic observables like pressure, temperature, heat capacity, stress tensor etc. are determined using statistical mechanics through time averages. The validity of this approach is based on the hypothesis that the system is ergodic so that time averages are equivalent to ensemble averages. One fundamental ensemble is called the micro-canonical ensemble and is characterized by constant number of particles N, constant volume V, and constant total energy E (NVE). Other examples include the canonical or NVT ensemble and the isothermal-isobaric or NPT ensemble (feasible by introducing a coupling to appropriate 'thermostats' and 'barostats') (Bin04).

Following this brief introduction, the report describes some preliminary actions that have been undertaken in view of a future involvement in this research area. As already anticipated, the focus of the document is on $(U,Pu)O_2$ fuel. MOX fuel is already used in commercial reactors and it is a fundamental issue for the potential

deployment of fast breeder reactors. A deep and sound knowledge of the thermophysical properties is crucial for its safe, reliable, and economic use. Therefore, MD offers a fruitful opportunity for the acquisition of knowledge and competence in a research area of great interest.

The report presents a review of the MD studies on PuO_2 and MOX fuel. This section aims at giving the state-of-the-art of MOX simulations providing information on codes, details of simulations, and topics most debated by the scientific community. The review is presented in Section 2. In Section 3, the potentials more frequently applied in the literature are briefly presented. In Section 4, the capabilities of the LAMMPS code are resumed. The code has been downloaded and installed. For testing purpose, preliminary calculations on the thermal conductivity of UO_2 have been performed. The presentation of this data has been postponed to a separate technical report under preparation.

2 MOLECULAR DYNAMICS LITERATURE: PuO_2 AND MOX FUEL

The work of Yamada et al. (2000) is one of the first studies dealing with the thermophysical properties of PuO_2 and MOX fuel (Yam00). The authors considered a system composed of 324 ions arranged in a CaF_2 type crystal structure. Calculations were performed in NPT and NVT ensembles. The thermal conductivity was calculated in the NPT ensemble by means of the Green-Kubo correlation.

The pair potential is partially ionic with a component that takes into account the cation-anion covalent bond. The authors present results about the lattice parameter, specific heat, compressibility, oxygen diffusivity, and thermal conductivity of PuO_2 (Yam00). The authors evaluated these quantities also in the case of MOX fuel. The analysis of $(U_{0.8}Pu_{0.2})O_2$ shows that the Bredig transition occurs in the specific heat and oxygen diffusivity at about 2350 K. With regard to the thermal conductivity of MOX fuel, the authors show results obtained at 360 K that suggest a decrease in conductivity with increasing plutonium content (Yam00). The behaviour of the thermal conductivity with temperature showed good agreement with the experimental data.

In (Kur01), MD calculations have been carried out on a low plutonium content MOX (20 at.%). Most of the hypotheses assumed in the analysis are quite consistent with the calculations described in (Yam00). Simulations have been performed in the temperature interval 300-2500 K while pressure ranges from 0.1 MPa up to 1.5 GPa. They employed the semi-empirical potential discussed in (Yam00). The authors calculated the thermal expansion, compressibility, heat capacity, and thermal conductivity of UO_2, PuO_2 and MOX. Results are in general good agreement with the values published in the open literature and confirm the existence of a premelting transition (2350 K). The occurrence of the Bredig transition was not confirmed in the case of PuO_2 (Kur01).

In (Ari05), the thermal properties of UO_2 and PuO_2 have been studied using two different pair potentials: Born–Mayer–Huggins (BMH) fully ionic and BMH partly ionic. The ionicity employed in the partially ionic model was 67.5%. The authors showed results of the lattice parameter and compressibility that supported the choice of the BMH-PIM pair potential. Based on this assumption, the specific heat and thermal conductivity have been evaluated (Ari05). Results showed some deviation between the predicted and experimental heat capacity of PuO_2. In their analysis, the thermal conductivity of UO_2 turned out to be lower than PuO_2. The accuracy seen in these results is better at high temperature while at low temperature (<500 K) the deviation of calculations is more significant. Authors argue that this effect could be due to impurities, lattice defects, grains boundaries that are not taken into account in calculations that consider a perfect crystal.

Arima et al. discussed the thermal conductivity of stoichiometric and hypo-stoichiometric MOX fuel (Ari06). This study intends to extend the analysis presented in (Yam00) and (Kur01) focusing on the effect of the O/M ratio on thermal conductivity. The temperature interval of interest is 300-2000 K. The authors applied the Born–Mayer–Huggins (BMH) potential with the partially ionic model. The ionicity of atomic bonds was 67.5%. The period used for the equilibration of the system was

40 ps. Thermal expansion and bulk modulus have been determined in the NPT ensemble. Thermal conductivity was determined in NVE (micro-canonical ensemble). The evaluations of the $(U_{0.8}Pu_{0.2})O_2$ lattice parameter and bulk modulus showed good agreement with the experimental data. The thermal conductivity has been tested in the interval of plutonium oxide concentration 0.0-30.0 mol.% with stoichiometry varying in the domain 1.94-2.00. The authors show a theoretical approach supporting the hypothesis that the concentration of plutonium has an impact on the thermal conductivity of MOX fuel. However, they conclude that in stoichiometric MOX this effect is small especially at high temperatures (Ari06). On the contrary, the effect of the O/M ratio on the thermal conductivity of $(U_{0.8}Pu_{0.2})O_2$ is pronounced especially at low temperature. Their calculations are in better agreement with the modelling presented in (Dur00) while the correlation given in (Phi92) seems to overestimate the effect of the O/M ratio predicted in simulations.

A series of MD calculations focused on MOX fuels containing americium oxide is presented in (Kur06). The effect of americium turned out to be not significant for the evaluation of thermal properties. Temperature and pressure have been controlled separately aiming to perform calculations in the NPT ensemble. The interatomic potential applied by the authors has been derived from the literature (Ida76). The ionicity was 60%. In the article, evaluations of the lattice parameter, heat capacity and thermal conductivity are presented. Results agree on the existence of Bredig transition in MOX fuel. This transition could explain the markedly increase in the heat capacity seen beyond 2000 K and the increase in the oxygen displacement around 2500 K (Kur06). The authors point out that the characteristics of americium are consistent with the limited effect noted in simulations. However, non-stoichiometry, atomic scale point defects, grain boundaries, cracks and pores may change the conclusions drawn in the case of perfect crystal lattice (Kur06).

The thermal properties and the mobility of oxygen defects of UO_2, PuO_2, and 30%-MOX have been calculated in (Ter07). The potential used for these calculations is modelled in the articles (Yam00; Kur01). The author confirms that the addition of PuO_2 in MOX decreases the thermal conductivity. Besides the verification of the capabilities of this pair potential to describe the thermal properties, the analysis is also focused on the effect of the addition of plutonium on the diffusion and energy migration of defects. In MOX, the diffusion coefficient of interstitials increases showing a different behaviour beyond 1500 K (Ter07).

In (Ari08), the authors apply the homogeneous non-equilibrium molecular dynamics (NEMD) comparing its outcomes with the indications of experiments and equilibrium molecular dynamics (EMD) simulations. The interatomic potential is coincident with the model used in previous studies (Ari06). The details of calculations are pretty much the same of those presented in previous studies. Their analysis deals with the thermal conductivity of MOX fuel as a function of temperature and stoichiometry (Ari08). Both methods agree on the fact that the thermal conductivity decreases with increasing deviation from stoichiometry. In comparison with stoichiometric UO_2, the addition of plutonium in MOX fuel has a limited effect. The use of NEMD proved to give results with better accuracy and lower computational costs.

Tiwary et al. (2011) developed an interatomic potential for MOX and advanced fuels. The potential is composed of a short-range term and a long-range term. The first one is based on the Ziegler-Biersack-Littmark (ZBL). Parameters have been fitted against a large database of *ab initio* calculations and experimental data (e.g., thermal expansion). The authors show MD results of PuO_2 and NpO_2. The results of lattice parameter and enthalpy proved in be in good agreement with the experimental measurements (Tiw11).

Basak and Kolokol (2012) adopt a pseudo-ion approach to discuss the thermophysical properties of MOX fuel. The radius and mass of plutonium and uranium cations are quite similar, for this reason, the authors judged that the average dynamic behaviour of MOX solid solution could be properly described though the use of a pseudo-ion. This choice reduces the inaccuracy due to the construction of the supercell through the random substitution of uranium with plutonium cations. The pseudo-ion resumes the physical properties of $U_{0.8}Pu_{0.2}$. The ionicity adopted in calculations is 60%. The authors discuss the inherent high temperature instability of the oxygen sub-lattice in fluorite-type structures (Bredig transition). This transition is often characterized by a sudden rise in the anionic diffusivity. Based on their simulations, the onset of the Bredig transition lies at a temperature around 2400 K. They claim that the use of a pseudo-ion approach avoids the scatter seen in the results obtained through a random construction of the MOX lattice permitting a more accurate determination of the temperature at which the Bredig transition occurs (Bas12). Evaluations of the lattice parameter, thermal expansion, isothermal compressibility, and specific heat proved to be in reasonable good agreement with the experimental data.

Nichenko and Staicu focus their analysis on the effect that plutonium concentration has on the thermal conductivity of MOX fuel (Nic13). First of all, the authors state that the experimental measurements of the thermal conductivity in the case of PuO_2 do not give consistent indications. Similarly, the review of MOX thermal conductivity results published in the literature does not permit to draw agreed conclusions. Therefore, a proper modelling of the separate effects of plutonium content, plutonium distribution and stoichiometry is still unfeasible (Nic13). They employ the potential developed in the studies of Arima et al. using a refined analytical treatment that considers a truncation of the Coulomb potential beyond cutoff. Authors propose a filtering of the heat current autocorrelation function to improve the evaluation of the thermal conductivity done by means of the Green-Kubo correlation. The isothermal-isobaric (NPT) statistical ensemble was applied to simulate the lattice at constant temperature and pressure (Berendsen thermostat and barostat). Their results indicate the existence of a minimum in MOX thermal conductivity at a plutonium concentration of 45 at.%. In this case, the thermal conductivity is about 14% lower than UO_2.

The article of Matsumoto et al. focuses on the effect of the O/M ratio on the thermal conductivity of MOX fuel containing a concentration in plutonium of 20 at.% (Mat13). Authors considered in their analysis the interval of O/M ratio 1.90-2.00. They determined the thermal conductivity through the Fourier's law using a non-equilibrium MD approach. The decrease due to the O/M ratio seen in the thermal conductivity is

significant especially at low temperature where the phonon-lattice scattering is dominant. Their evaluations are in in agreement with the indications given in (Phi92). Results tend to underestimate the predictions of the Duriez's correlation (Dur00). At a given level of stoichiometry, the addition of plutonium degrades the thermal conductivity of MOX fuel (Mat13).

Ma et al. studied the effect of the O/M ratio on the thermal conductivity of $(U_{0.75}Pu_{0.25})O_{2-x}$ (Ma14). In addition, they showed evaluations of the lattice parameter, compressibility, and thermal expansion. Besides the consideration of the O/M ratio, they discussed the effect of plutonium content on the thermal conductivity of a stoichiometric MOX (plutonium concentration 15-30 at.%). Their results confirm previous experimental indications and show that the O/M ratio has a significant effect on the lattice parameter and the linear thermal expansion coefficient. In this latter case, this statement is valid especially at high temperatures. Their evaluations on the thermal conductivity of MOX fuel support the hypothesis that the effect of plutonium concentration is by far lower than the deviation from stoichiometry. However, the consistency of the results with the experimental data is confirmed by the authors in the low temperature and for values of the O/M ratio higher than 1.94 (Ma14).

Cooper et al. proposed an alternative potential for the description of the properties of actinide oxides (Coo14). The authors employ a many-body potential using the embedded atom method (EAM). This new potential adopts a semi-empirical approach that determines the parameters used in calculations by fitting the experimental data of material properties. This model is composed of two parts: the first one deals with a pair potential where coulombic, Buckingham, and Morse terms are applied; the second is a contribution depending on the simultaneous interaction with all ions (many-body). The pair potential contribution remains dominant where a cutoff is used to avoid that the many-body interaction could overcome the effect of the short-range forces. The model adopts a ionicity of 56%. This model, mostly developed on the thermal expansion experimental data, has been applied to predict the specific heats and bulk moduli as a function of temperature (Coo14). The evaluations presented in this article, in good agreement with the literature, deal with the following actinide oxides: AmO_2, CeO_2, CmO_2, NpO_2, PuO_2, ThO_2 and UO_2. In addition, the authors discuss the evaluations of the UO_2 melting temperature and the energy needed for the formation of defects (Coo14).

In (Liu15), the authors aim at discussing the MOX thermal conductivity as a function of PuO_2 concentration. For the purpose, they apply a non-equilibrium MD approach. The temperature profiles of the calculated gradients are then averaged to determine the thermal conductivity. The positions of plutonium ions are randomly distributed in the uranium sub-lattice. Their results support the hypothesis that the thermal conductivity of PuO_2 is higher than UO_2 at 300 K while they are comparable at higher temperature. These results do not take into account the spin-phonon scattering in UO_2. The reduction in the thermal conductivity of $(U_{0.5}Pu_{0.5})O_2$ at 300 K is estimated between 11% and 20% in comparison with the thermal conductivity of pure components (Liu15). In general, the thermal conductivity of MOX turned out to be smaller than the pure components. The absolute deviations decrease with increasing temperature. The use of the EAM potential gave values generally lower than the

Buckingham potential, however, the indications given by these two different hypotheses are in general good agreement. The use of the EAM potential confirms the decrease of MOX thermal conductivity at 300 K (11%). The decrease becomes insignificant at higher temperatures. At low temperature, the difference in lattice parameter and mass has an impact in the phonon-lattice scattering mechanism. In their analysis, the inclusion of the spin scattering, has a significant impact on the thermal conductivity of UO_2 that turns out to be much lower than PuO_2. As such, the addition of plutonium has a beneficial effect on the thermal conductivity of MOX fuel that now increases in comparison with the thermal conductivity of UO_2.

Matsumoto et al. employ a non-equilibrium molecular dynamics (NEMD) approach to determine the thermal conductivity of UO_2, PuO_2, and MOX fuel (Mat15). The authors evaluate these quantities using the Busing-Ida pair potential with a ionicity of 67.5%. The thermal conductivity decreases with increasing supercell length. Their results agree on the hypothesis that the thermal conductivity of MOX fuel is comparable with UO_2 and lower than PuO_2. However, the effect of the addition of PuO_2 is small (Mat15). According to these results, the thermal conductivity of PuO_2 is higher than UO_2. Their results are in satisfactory agreement with the experimental measurements in the whole range of temperature considered in the study.

In (Coo15a), the authors study the degradation of the thermal conductivity of MOX fuel by means of non-equilibrium MD simulations. The topic of the article is on the effect of plutonium concentration. This quantity is studied in the interval 0.0-100.0 at.%. The authors use a potential that includes a many-body contribution besides the pair potential term (Coo14, Coo14b). Results indicate that the thermal conductivity of plutonium dioxide is higher than uranium dioxide. The addition of plutonium has a little effect on the thermal conductivity of uranium oxide. A minimum in the thermal conductivity is noted at a concentration of uranium of 75 at.% rather than 50 at.%. Inhomogeneity in plutonium distribution has a positive effect on the thermal conductivity but this effect should be compared with the effects of the phenomena occurring under irradiation (Coo15a).

Cooper et al. studied the thermophysical properties of the $(U_xPu_{1-x})O_2$ system (Coo15b). The interval of temperature of interest is 300-3200 K considering 3 concentrations of plutonium (25, 50, 75 at.%). Their analysis is focused on the lattice parameter, linear thermal expansion coefficient, enthalpy and specific heat at constant pressure as a function of temperature. The diffusivity of oxygen is also discussed. The authors applied the many-body potential presented in (Coo14). For the purpose, the parameters of the PuO_2 model have been refined to achieve a better agreement with the experimental data of melting temperature. The tuning of coefficients caused a decrease in predictions down to an interval 2750-2850 K much more consistent with the experimental findings. In this article, the energy characterisation of oxygen defects is discussed as well. The introduction of defects in the supercell is carried out once the system energy has been minimized. An evaluation of the enthalpy of the defective supercell is then carried out. The comparison of this quantity with an ideal supercell has been used to determine the enthalpies of oxygen vacancies and interstitials. In calculations, 10 supercells are randomly generated and their results averaged. The results of the lattice parameter

and thermal expansion show a deviation from the Vergard's law at high temperature. In addition, an influence of the concentration of plutonium is noted, however, the authors underline that these results are not validated because of lacking in the experimental data (available up to 1700 K). The behaviour of the thermal expansion noted at high temperature is confirmed in the simulations of the enthalpy and specific heat. The enthalpy increment as a function of temperature increases more significantly between 2000 and 3000 K (Coo15b). Similarly, the results of oxygen diffusivity confirm the existence of a superionic transition. The increase in uranium concentration leads to an increase in the temperature of transition. The authors note that the diffusivity of oxygen in MOX fuel is higher than the interpolation of the values corresponding to the pure components. Based on these results an enhanced diffusivity of oxygen is predicted at the level of fuel temperatures used in operating reactors.

In (Gho16), the melting temperature, enthalpy increments, and density of solid and liquid ThO_2, UO_2, and PuO_2 are studied. Authors employ the many-body potential described in (Coo14) and (Coo15b). Different strategies have been applied for the creation of the initial supercell where a random substitution of atoms is considered. The melting temperature was determined by means of a two-phase supercell where half of it is initially in the solid phase while the other is in the liquid phase. The melting temperature was estimated setting a final temperature at which the supercell turns to a single phase system. The melting temperature of PuO_2 was estimated lying in the interval 2800-2825 K. The agreement noted between calculations and experimental values up to high temperatures confirms the capability of the applied potential to be used for the simulation of MOX fuel (Gho16).

The information published in the literature has been resumed in Tab. 2.1 and 2.2. Tables contain the information dealing with MOX fuel published within a specific article and do not resume all the information provided by the authors.

Reference	Fuel	Temperature (K)	Code	Property	Potential
Yamada, 2000	PuO_2 $(U_{1-x}Pu_x)O_2$ x 0.0-1.0	300-2500	MXDRTO	LP, SH, COM, OD, TC	BMH-PIM MORSE
Kurosaki, 2001	PuO_2 $(U_{0.8}Pu_{0.2})O_2$	300-2500	MXDRTO	TE, COM, SH, TC	BMH-PIM MORSE
Arima, 2005	PuO_2	300-2000	MXDRTO	LP, COM (bulk modulus) , SH, TC	BMH-FIM BMH-PIM
Arima, 2006	$(U_{1-x}Pu_x)O_{2-y}$ x 0.1, 0.2, 0.3 (y=0.0) y 0.02, 0.04, 0.06 (x=0.2)	300-2000	MXDRTO	LP, TE, COM, bulk modulus, TC	BMH-PIM
Kurosaki, 2006	$(U_{0.7-x}Pu_{0.3}Am_x)O_2$ x 0, 0.016, 0.03, 0.05, 0.10, 0.15	300-2500	MXDRTO	LP, HC, TC	BMH-PIM MORSE
Terentyev, 2007	PuO_2 $(U_{0.7}Pu_{0.3})O_2$	300-2500	MOLDY	LP, HC, TC, TE, OD	BMH-PIM MORSE
Arima, 2008	$(U_{0.8}Pu_{0.2})O_{2-y}$ y 0, 0.02, 0.04, 0.06	300-2000	MXDRTO	TC	BMH-PIM
Tiwary, 2011	PuO_2, NpO_2	500-1300	-	LP, E	ZBL + long-range term
Basak, 2012	$(U_{0.8}Pu_{0.2})O_2$	300-3000	MOLDY	LP, TE, SH, OD, COM	BMH-PIM MORSE
Nichenko, 2013	$(U_{1-x}Pu_x)O_2$ x 0.0-1.0	300-1600	-	LP, TC	BMH-PIM MORSE
Matsumoto, 2013	$(U_{0.8}Pu_{0.2})O_{2-x}$ x 0.0, 0.02, 0.04, 0.10	300-2000	MXDRTO	TC	BMH-PIM
Cooper, 2014	PuO_2	300-3000	LAMMPS	bulk modulus, SH	Many-body EAM
Ma, 2014	$(U_{0.75}Pu_{0.25})O_{2-y}$ y 0.0, 0.02, 0.06, 0.10, 0.15, 0.20, 0.25 $(U_{1-x}Pu_x)O_2$ x 0.15, 0.20, 0.25, 0.30	300-3000	LAMMPS	LP, TE, COM, bulk modulus, TC	BMH-PIM

Quantities (MT=melting temperature; E=enthalpy; D=density; LP=lattice parameter; TE=thermal expansion; COM=compressibility; TC=thermal conductivity; SH=specific heat; OD=oxygen diffusivity; HC=heat capacity)

Table 2.1: PuO_2 and MOX literature

Liu, 2015	$(U_{1-x}Pu_x)O_2$ x 0.0, 0.25, 0.50, 0.75, 1.0	300-1500	LAMMPS	TE, TC	BMH-FIM Many-body EAM
Matsumoto, 2015	PuO_2 $(U_{0.8}Pu_{0.2})O_2$	300-2000	MXDRTO	TC	BMH-PIM
Cooper, 2015a	$(U_xPu_{1-x})O_2$ x 0.0, 0.25, 0.50, 0.75, 1.0	300-2000	LAMMPS	TC	Many-body EAM
Cooper, 2015b	$(U_xPu_{1-x})O_2$ x 0.0, 0.25, 0.50, 0.75, 1.0	300-3200	LAMMPS	LP, TE, E, SH, OD	Many-body EAM
Ghosh, 2016	PuO_2	300-6000	LAMMPS	MT, E, D	Many-body EAM

Quantities (MT=melting temperature; E=enthalpy; D=density; LP=lattice parameter; TE=thermal expansion; COM=compressibility; TC=thermal conductivity; SH=specific heat; OD=oxygen diffusivity; HC=heat capacity)

Table 2.1 (continued): PuO_2 and MOX literature

3 INTERATOMIC POTENTIALS

The review presented in previous section has shown that few types of potentials are applied in simulations. In this section, a brief description of the interatomic potentials discussed in the literature is given. All the correlations are featured by a number of parameters that are usually fitted on the experimental data of specific properties such as the lattice parameter, bulk modulus, elastic properties etc. Therefore, the models used in MD are referred as semi-empirical potentials. They aim at reproducing the force field existing among the elementary compounds of the materials under consideration (atoms, ions).

The model mentioned in Tab. 2.1 as BMH-PIM is presented in Eq. 1. It is the partial ionic model of the Born-Mayer-Huggins pair potential (BMH). The first term accounts for the long-range Coulomb potential, the following two terms corresponds to the short-range interactions due to Pauli repulsion and van der Waals. In this correlation the f_0 coefficient is an empirical parameter used to adjust the model. The parameters z_i and z_j are the effective electronic charges according to the level of ionicity adopted for the description of the atomic bonds. Finally, r_{ij} is the distance between atom *i* and atom *j*. The remaining parameters (*a*, *b*, *c*) are fitted on the experimental data and are specific of the type of atoms/ions interacting. In the studies of MOX fuel, these coefficients are referring to the fuel components: oxygen, uranium, and plutonium. If the fuel is hypostoichiometric the different valence of cations should be properly considered.

$$U_{ij}(r_{ij}) = \frac{z_i z_j e^2}{r_{ij}} + f_0(b_i + b_j)\exp\left(\frac{a_i + a_j - r_{ij}}{b_i + b_j}\right) - \frac{c_i c_j}{r_{ij}^6} \qquad (1)$$

Reference	Ions	Ensembles	Equilibration (Calculation) (ps)	Time step (fs)	Coefficients
Yamada, 2000	324	NPT, NVT	20	2	literature and fitting LP, TE
Kurosaki, 2001	324	NPT, NVT	20	2	Literature and fitting LP(T, P)
Arima, 2005	324	NPT, NVE	40 (40 and 1000 for TC in NVE)	2	literature and fitting TE, COM at room temperature
Arima, 2006	324	NPT, NVE	40 (40 and 1000 for TC in NVE)	2	literature and fitting TE, COM (Pu^{3+})
Kurosaki, 2006	768	NPT	20	2	literature
Terentyev, 2007	40500	NVT, NPT	10 (15)	0.5	literature
Arima, 2008	324	NVE (EMD)	40 (1000)	2	literature
Tiwary, 2011	324	NPT	10 (100)	<1 >0.5	GGA + U ab initio and experimental TE
Basak, 2012	12000	NPT, NVT	20	1	Literature and fitting of lattice parameter at 300, 800, 1300, 1800 K
Nichenko, 2013	2592	NPT	-	-	literature
Matsumoto, 2013	4320	NPT	40 (1000 for TC in NPT)	2	literature
Cooper, 2014	768	NPT	16 (4)	0.2	Fitting LP, elastic constants, bulk modulus, TE
Ma, 2014	2592	NPT, NVT	-	-	literature
Liu, 2015	-	NPT (thermal expansion) NVE	100 (13000)	-	literature
Matsumoto, 2015	4320-17280	NPT (0.1 MPa)	-	2	literature
Cooper, 2015a	4500-72000	-	-	-	literature
Cooper, 2015b	12000	NPT NVT (for OD)	20 (4; 1000 for OD)	2 (1 for OD)	Literature, refitting based on PuO_2 MT
Ghosh, 2016	12000, 15552 (for MT)	NPT	40 (10)	2	literature

Table 2.2: PuO_2 and MOX literature

The Born–Mayer–Huggins potential used in the fully ionic model (BMH-FIM) is presented in Eq. 2. The second term represents Pauli repulsion, the third term the short-range van der Waals interaction. In the Coulomb term, the full electronic charges should be considered. The meaning of symbols is coincident with the previous description where A_{ij}, ρ_{ij}, and C_{ij} are the empirical coefficients of the interacting pair of ions.

$$U_{ij}(r_{ij}) = \frac{z_i z_j e^2}{r_{ij}} + A_{ij} \exp\left(-\frac{r_{ij}}{\rho_{ij}}\right) - \frac{C_{ij}}{r_{ij}^6} \quad (2)$$

The covalent part of the atomic bond is modelled by means of the Morse potential (Eq. 3). It is applied only to cation–anion pairs and r_{ij}^* is the anion–cation bond length. In this equation, D_{ij} and β_{ij} denote the depth and the shape of the potential. Eq. 1 and Eq. 3 are applied together to form the potential BMH-PIM MORSE in Tab. 2.1.

$$U_{ij}(r_{ij}) = D_{ij}\left\{\exp\left[-2\beta_{ij}(r_{ij} - r_{ij}^*)\right] - 2\exp\left[-\beta_{ij}(r_{ij} - r_{ij}^*)\right]\right\} \quad (3)$$

Finally, the potential developed by Cooper et al. (2014) is shown in Equations 4, 5, 6, and 7. This potential is indicated in Tab. 2.1 as many-body EAM potential. As presented in Eq. 4, the potential is composed of one term expressing the pair component while the second term accounts for many-body interactions. The pair potential is composed of three terms: Coulomb, Buckingham, and Morse potentials to describe short- and long-range interactions (Eq. 5). The analytical expression of the first two terms of the pair potential is presented in Eq. 6. With regard to previous indications, an effective ionicity is applied in the definition of the ionic charges. The term expressing the covalent part of the atomic bonds $\Phi^{(M)}$ is consistent with the correlation presented in Eq. 3.

$$E_i = \frac{1}{2}\sum_j \Phi_{\alpha\beta}(r_{ij}) - G_\alpha\left(\sum_j \sigma_\beta(r_{ij})\right)^{1/2} \quad (4)$$

$$\Phi_{\alpha\beta}(r_{ij}) = \Phi_{\alpha\beta}^{(C)}(r_{ij}) + \Phi_{\alpha\beta}^{(B)}(r_{ij}) + \Phi_{\alpha\beta}^{(M)}(r_{ij}) \quad (5)$$

$$\Phi_{\alpha\beta}^{(C)}(r_{ij}) + \Phi_{\alpha\beta}^{(B)}(r_{ij}) = \frac{z_\alpha z_\beta}{4\pi\varepsilon_0 r_{ij}} + A_{\alpha\beta}\exp\left(-\frac{r_{ij}}{\rho_{\alpha\beta}}\right) - \frac{C_{\alpha\beta}}{r_{ij}^6} \qquad (6)$$

The embedding function accounting for the many-body perturbation is proportional to the square root of the sum of the contributions described in Eq. 7. G_α is the constant of proportionality. This effect is a function of the inverse of the 8-th power of the distance between ions where n_β is an empirical coefficient. A short range cut-off at 1.5 angstrom is applied to avoid that the forces due to the EAM term could overcome the short-range pair repulsion (Coo14).

$$\sigma_\beta(r_{ij}) = \frac{n_\beta}{r_{ij}^8} \qquad (7)$$

4 LAMMPS CODE

The LAMMPS code (Large-Scale Atomic/Molecular Massively Parallel Simulator) is one of the three codes used in the literature presented in Section 2. Therefore, it has the capabilities suitable for the analysis of MOX fuel. The code has been downloaded and a stand-alone version for WINDOWS has been installed and applied to the calculation of UO_2 thermal conductivity by means of the Green-Kubo correlation. The results of this initial testing phase will be presented in a report under preparation.

LAMMPS is a classical molecular dynamics code capable of modelling an ensemble of particles in a liquid, solid, or gaseous state. It can model atomic, polymeric, biological, metallic, granular, and coarse-grained systems using a variety of force fields and boundary conditions (Pli95).

The code runs on single-processor machines, but it is designed for parallel computing on any parallel machines with a C++ compiler and supporting the message passing interface (MPI). LAMMPS is a freely-available open-source code distributed under the terms of the GNU Public License, The code was originally developed under the US Department of Energy CRADA (Cooperative Research and Development Agreement) in collaboration with three private companies. It is now distributed by the Sandia National Laboratories.

LAMMPS integrates the Newton's equations of motion for collections of atoms, molecules, or macroscopic particles that interact via short- or long-range forces with a variety of initial and/or boundary conditions. The code uses lists of neighbors to keep track of nearby particles. The lists are optimized for systems with particles that are repulsive at short distances, so that the local density of particles never becomes too large.

Some key features of the code are briefly listed.

Particles and model types

- atoms;
- coarse-grained particles (e.g. bead-spring polymers);
- united-atom polymers or organic molecules;
- metals;
- granular materials;
- coarse-grained mesoscale models;
- finite-size spherical and ellipsoidal particles;
- finite-size line segment (2d) and triangle (3d) particles;
- point dipole particles;
- rigid collections of particles;
- hybrid combinations of these.

Force fields

- pairwise potentials: Lennard-Jones, Buckingham, Morse, Born-Mayer-Huggins, Yukawa, soft, class 2 (COMPASS), hydrogen bond, tabulated;
- charged pairwise potentials: Coulombic, point-dipole;
- many-body potentials: EAM, Finnis/Sinclair EAM, modified EAM (MEAM), embedded ion method (EIM), EDIP, ADP, Stillinger-Weber, Tersoff, REBO, AIREBO, ReaxFF, COMB, SNAP, Streitz-Mintmire, 3-body polymorphic;
- long-range interactions for charge, point-dipoles, and LJ dispersion: Ewald, Wolf, PPPM;
- polarization models: QEq, core/shell model, Drude dipole model;
- charge equilibration: QEq via dynamic, point, shielded, Slater methods;
- coarse-grained potentials: DPD, GayBerne, REsquared, colloidal, DLVO;
- mesoscopic potentials: granular, Peridynamics, SPH;
- electron force field: eFF, AWPMD;
- bond potentials: harmonic, FENE, Morse, nonlinear, class 2, quartic (breakable);
- angle potentials: harmonic, CHARMM, cosine, cosine/squared, cosine/periodic, class 2 (COMPASS);
- dihedral potentials: harmonic, CHARMM, multi-harmonic, helix, class 2 (COMPASS), OPLS;
- improper potentials: harmonic, cvff, umbrella, class 2 (COMPASS);
- polymer potentials: all-atom, united-atom, bead-spring, breakable;
- water potentials: TIP3P, TIP4P, SPC;
- implicit solvent potentials: hydrodynamic lubrication, Debye;
- force-field compatibility with common CHARMM, AMBER, DREIDING, OPLS, GROMACS, COMPASS options;
- access to KIM archive of potentials via pair kim;
- hybrid potentials: multiple pair, bond, angle, dihedral, improper potentials can be used in one simulation;

- overlaid potentials: superposition of multiple pair potentials.

Atom creation

- read in atom coords from files;
- create atoms on one or more lattices (e.g., grain boundaries);
- delete geometric or logical groups of atoms (e.g. voids);
- replicate existing atoms multiple times;
- displace atoms.

Ensembles, constraints, and boundary conditions

- 2d or 3d systems;
- constant NVE, NVT, NPT, NPH, Parinello/Rahman integrators;
- thermostatting options for groups and geometric regions of atoms;
- pressure control via Nose/Hoover or Berendsen barostatting in 1 to 3 dimensions;
- simulation box deformation (tensile and shear);
- rigid body constraints;
- Monte Carlo bond breaking, formation, swapping;
- atom/molecule insertion and deletion;
- walls of various kinds;
- non-equilibrium molecular dynamics (NEMD);
- variety of additional boundary conditions and constraints.

5 CONCLUSIONS

The report presents some preliminary actions aimed at a future use of the Molecular Dynamics methodology for the study of MOX fuel. For the purpose, a review of the literature has been carried out. The MD simulations of MOX fuel published in the literature are resumed. The review has indicated a set of codes, interatomic potentials, and simulations details specific for the analysis of MOX fuel.

This has permitted to determine the domain in which MOX fuel have been investigated by the scientific community. Based on these indications, most of the possible applications of MD recalled in (NEA15) have not yet been exploited in the case of MOX fuel. Among the codes mentioned in the literature, the LAMMPS code has been used in many recent studies. In addition, the code is freely-available making simpler the perspective of a deeper involvement in this field of research. For this reason, the code has been downloaded and preliminary simulations performed.

These initial steps have confirmed the importance of the methodology, its current use in the study of MOX fuel and its future application as a realistic opportunity. However, it is also confirmed the efforts needed to achieve an adequate level of knowledge and competence. It is expected that in the near future, new steps forwards will be accomplished.

6 REFERENCES

[Ack11] Ackland G.J., D'Mellow K., Daraszewicz S.L., Hepburn D.J., Uhrin M., Stratford K., 2011, The MOLDY short-range molecular dynamics package, Computer Physics Communications 182, 2587–2604.

[Ari05] Arima T., Yamasaki S., Inagaki Y., Idemitsu K., 2005, Evaluation of thermal properties of UO_2 and PuO_2 by equilibrium molecular dynamics simulations from 300 to 2000K, Journal of Alloys and Compounds 400, 43–50.

[Ari06] Arima T., Yamasaki S., Inagaki Y., Idemitsu K., 2006, Evaluation of thermal conductivity of hypostoichiometric $(U,Pu)O_{2-X}$ solid solution by molecular dynamics simulation at temperatures up to 2000 K, Journal of Alloys and Compounds 415, 43–50.

[Ari08] Arima T., Yamasaki S., Idemitsu K., Inagaki Y., 2008, Equilibrium and nonequilibrium molecular dynamics simulations of heat conduction in uranium oxide and mixed uranium–plutonium oxide, Journal of Nuclear Materials 376, 139–145.

[Bas12] Basak C.B., Kolokol A.S., 2012, A Novel Pseudo-Ion Approach in Classical MD Simulation: A Case Study on $(U_{0.8}Pu_{0.2})O_2$ Mixed Oxide, Journal of the American Ceramic Society 95 [4], 1435–1439.

[Bin04] Binder K., Horbach J., Kob W., Paul W., Varnik F., 2004, Molecular dynamics simulations. Journal of Physics: Condensed Matter 16, S429–S453.

[Coo14] Cooper M.W.D., Rushton M.J.D., Grimes R.W., 2014, A many-body potential approach to modelling the thermomechanical properties of actinide oxides, Journal of Physics: Condensed Matter 26, 105401–105411.

[Coo15a] Cooper M.W.D., Middleburgh S.C., Grimes R.W., 2015, Modelling the thermal conductivity of $(U_xTh_{1-x})O_2$ and $(U_xPu_{1-x})O_2$, Journal of Nuclear Materials 466, 29–35.

[Coo15b] Cooper M.W.D., Murphy S.T., Rushton M.J.D., Grimes R.W., 2015, Thermophysical properties and oxygen transport in the $(U_x,Pu_{1-x})O_2$ lattice, Journal of Nuclear Materials 461, 206–214.

[Dur00] Duriez C., Alessandri J.-P., Gervais T., Philipponneau Y., 2000, Thermal conductivity of hypostoichiometric low Pu content $(U,Pu)O_{2-x}$ mixed oxide, Journal of Nuclear Materials 277, 143–158.

[Gho16] Ghosh P.S., Kuganathan N., Galvin C.O.T., Arya A., Dey G.K., Dutta B.K., Grimes R.W., 2016, Melting behavior of $(Th,U)O_2$ and $(Th,Pu)O_2$ mixed oxides, Journal of Nuclear Materials 479, 112–122.

[Ida76] Ida Y., 1976, Interionic Repulsive Force and Compressibility of Ions, Physics of the Earth and Planetary Interiors 13, 97–104.

[Kur01] Kurosaki K., Yamada K., Uno M., Yamanaka S., Yamamoto K., Namekawa T., 2001, Molecular dynamics study of mixed oxide fuel, Journal of Nuclear Materials 294, 160–167.

[Kur06] Kurosaki K., Adachi J., Katayama M., Osaka M., Tanaka K., Uno M., Yamanaka S., 2006, Molecular Dynamics Studies of Americium-Containing Mixed Oxide Fuels, Journal of Nuclear Science and Technology 43(10), 1224–1227.

[Liu15] Liu X.-Y., Cooper M.W.D., Stanek C.R., Andersson D.A., 2015, The thermal conductivity of mixed fuel $U_xPu_{1-x}O_2$: molecular dynamics simulations, LA-UR-15-28079, Los Alamos Laboratories, Los Alamos, NM, USA.

[Ma14] Ma J., Zheng J., Wan M., Du J., Yang J., Jiang G., 2014, Molecular dynamical study of physical properties of $(U_{0.75}Pu_{0.25})O_{2-x}$, Journal of Nuclear Materials 452, 230–234.

[Mat13] Matsumoto T., Arima T., Inagaki Y., Idemitsu K., Kato M., Uchida T., 2013, Investigation of O/M ratio effect on thermal conductivity of oxide nuclear fuels by non-equilibrium molecular dynamics calculation, Journal of Nuclear Materials 440, 580–585.

[Mat15] Matsumoto T., Arima T., Inagaki Y., Idemitsu K., Kato M., Uchida T., 2015, Molecular dynamics calculations of heat conduction in actinide oxides under thermal gradient, Progress in Nuclear Energy 85, 271–276.

[NEA15] State-of-the-Art Report on Multi-scale Modelling of Nuclear Fuels, 2015, NEA/NSC/R/(2015)5, OECD/Nuclear Energy Agency, Paris.

[Nic13] Nichenko S., Staicu D., 2013, Molecular Dynamics study of the mixed oxide fuel thermal conductivity, Journal of Nuclear Materials 439, 93–98.

[Phi92] Philipponneau Y., 1992, Thermal conductivity of $(U,Pu)O_{2-x}$ mixed oxide fuel, Journal of Nuclear Materials 188, 194–197.

[Pli95] Plimpton S., 1995, Fast Parallel Algorithms for Short-Range Molecular Dynamics, Journal of Computational Physics 117, 1-19.

[Ter07] Terentyev D., 2007, Molecular dynamics study of oxygen transport and thermal properties of mixed oxide fuels, Computational Materials Science 40, 319–326.

[Tiw11] Tiwary P., van de Walle A., Jeon B., Grønbech-Jensen N., 2011, Interatomic potentials for mixed oxide and advanced nuclear fuels, Physical Review B 83, 094104-1 to -6.

[Uff15] Van Uffelen P., 2015, Use of advanced simulations in fuel performance codes, NEA/NSC/R/(2015)5, OECD/Nuclear Energy Agency, 352–358.

[Yam00] Yamada K., Kurosaki K., Uno M., Yamanaka S., 2000, Evaluation of thermal properties of mixed oxide fuel by molecular dynamics, Journal of Alloys and Compounds 307, 1–9.